Development of Thin-Film Composite forward Osmosis Hollow Fiber Membranes Using Direct Sulfonated Polyphenylenesulfone (sPPSU) as Membrane Substrates

ARTICLE *in* ENVIRONMENTAL SCIENCE & TECHNOLOGY · JUNE 2013

Impact Factor: 5.33 · DOI: 10.1021/es4013273 · Source: PubMed

Environmental Science & Technology

Article

pubs.acs.org/est

Development of Thin-Film Composite forward Osmosis Hollow Fiber Membranes Using Direct Sulfonated Polyphenylenesulfone (sPPSU) as Membrane Substrates

Peishan Zhong,[†,‡] Xiuzhu Fu,[‡] Tai-Shung Chung,[‡,*] Martin Weber,[§] and Christian Maletzko[∥]

[†]Functionalized Materials and Nanostructures, Global Research Center Singapore (A-GMM/F), BASF South East Asia Pte Ltd 61 Science Park Road, Singapore 117525

[‡]Department of Chemical & Biomolecular Engineering, National University of Singapore, 10 Kent Ridge Crescent, Singapore 119260

[§]Advanced Materials & Systems Research, Performance Materials, BASF SE GMV/W-B1, 67056 Ludwigshafen, Germany

[∥]Performance Materials, BASF SE G-PMS/PS-F206, 67056 Ludwigshafen, Germany

Supporting Information

ABSTRACT: This study investigates a new approach to fabricate thin-film composite (TFC) hollow fiber membranes via interfacial polymerization for forward osmosis (FO) applications. Different degrees of sulfonation of polyphenylenesulfone (PPSU) were adopted as membrane substrates to investigate their impact on water flux. It has been established that the degree of sulfonation plays a role in both creating a macrovoid-free structure and inducing hydrophilicity to bring about higher water fluxes. The fabricated membranes exhibit extremely high water fluxes of 30.6 and 82.0 LMH against a pure water feed using 2.0 M NaCl as the draw solution tested under FO and pressure retarded osmosis (PRO) modes, respectively, while maintaining low salt reverse fluxes below 12.7 gMH. The structural parameter (S) displays remarkable decreases of up to 4.5 times as the membrane substrate is switched from a nonsulfonated to sulfonated one. In addition, the newly developed TFC-FO membranes containing 1.5 mol % sPPSU in the substrate achieves a water flux of 22 LMH in seawater desalination using a 3.5 wt % NaCl model solution and 2.0 M NaCl as the draw solution under the PRO mode. To the best of our knowledge, this value is the highest ever reported for seawater desalination using flat and hollow fiber FO membranes. The use of sulfonated materials in the FO process opens up a frontier for sustainable and efficient production of potable water.

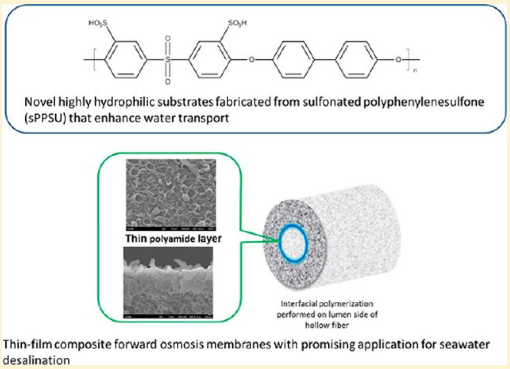

Thin-film composite forward osmosis membranes with promising application for seawater desalination

INTRODUCTION

Water scarcity in the 21st century is a pressing global issue[1,2] and forward osmosis has attracted much attention as an emerging technology[3,4] to alleviate this problem. It also brings about potential applications including power generation,[5,6] wastewater treatment, food processing,[7,8] and protein enrichment.[9] There are many advantages of the forward osmosis process which include requiring much less energy to induce a net flow of water in comparison with the traditional water treatment process such as reverse osmosis (RO) and low membrane fouling.[10−12] The use of an osmotic pressure gradient also helps reduce the use of depleting fuel sources which has brought about detrimental environmental problems to our earth.

The current dominant FO membrane in the commercial application comes from Hydration Technology Inc. (HTI). However, these membranes are cellulose-based and face problems such as degradation by microorganisms, narrow pH working range and low salt rejection. In contrast, the polyamide thin film composite (TFC) membrane fabricated from interfacial polymerization upon a suitable substrate is an attractive technique to mitigate the mentioned problems. This technique has been widely applied in the reverse osmosis (RO) process[13,14] and its concept has been extended to the FO process. Many studies have worked on the flat sheet[15−17] configuration while few studies have investigated TFC membranes in the hollow fiber configuration.[18−20]

The key prerequisites for the development of desirable TFC membranes for FO include (1) ultrathin semipermeable active layer with low water transport resistance and high salt rejection; (2) highly porous and thin supporting layer to minimize internal concentration polarization (ICP); (3) low fouling propensity and (4) sufficiently high mechanical strength.[10] These fundamental requirements have to be met in order to meet and achieve the attractive qualities, offered by the forward osmosis process. However, to date, the development of forward osmosis encounters the challenge of ineffective membranes that

Received: March 26, 2013
Revised: May 31, 2013
Accepted: June 3, 2013
Published: June 3, 2013

dx.doi.org/10.1021/es4013273 | Environ. Sci. Technol. 2013, 47, 7430−7436

play the critical role in most FO processes.[11] Hence, there is a need to search for suitable materials. These materials are preferred to be hydrophilic.[21]

In this work, direct sulfonated polyphenylenesulfone (sPPSU) with different concentrations of sulfonated monomer (sDCDPS), that is, 1.5 and 2.5 mol %, were applied as substrates for FO membranes. The objectives of this study is to (1) investigate the effect of sulfonation degree on the morphology of hollow fiber substrates spun from different spinning parameters; (2) explore the effect of sulfonation degree of the TFC membrane substrate on FO performance; and (3) explore their potential for seawater desalination. It has been postulated that an increase in hydrophilicity of membrane substrates would increase the FO water flux of these membranes and provide a solution to the current issues faced in the FO process.

A study by Shi et al has investigated the effect of substrate structure on the formation of the TFC layer upon it and concluded that the substrate should possess an MWCO of less than 300 kDa in order to achieve a desirable semipermeable skin.[22] Therefore, the MWCO of the substrates fabricated in this work will be controlled within the desirable range. The concentration of the PEG400 which acts as a pore former was varied in this work and the optimal condition was used.

In this work, hollow fibers with an inner selective layer were designed due to advantages which include (1) feed being able to be delivered into the lumen equally, (2) easy protection of the defect-free separation layer, and (3) low transport resistance in the permeate side.[23] The formulation of the dope to yield a macrovoid-free structure was also explored as macrovoids are viewed as mechanically weaker points on the membrane. The effect of PEG400 and the addition of water to the dope solution for macrovoid suppression were studied along with the spinning parameters.

MATERIALS AND METHODS

Materials. Polyphenylenesulfone (PPSU), 1.5 mol % and 2.5 mol % sulfonated polyphenylenesulfone (sPPSU) were used as the materials for the fabrication of various membrane substrates. The sPPSU materials were synthesized via the direct sulfonation synthesis route developed by McGrath et al.[24] The 1.5 mol % and 2.5 mol % sPPSU have IEC values of 5.1 and 8.2 meq/100g polymer. N-methyl-2-pyrrolidone (NMP) and polyethylene glycol 400 (PEG400) from Merck were used as the solvent and pore former in the dope solution preparation, respectively. More information on the chemicals used for interfacial polymerization can be found in the Supporting Information (SI).

Cloud Point Measurements. To determine the binodal composition of the PPSU/PEG400/NMP/water system, cloud point data were obtained by means of a titration method. It is known that a dope formulation near to the binodal curve will result in membranes with macrovoid-free structures upon phase inversion.[25,26] Distilled water was slowly added to the system of polymer, additive, and solvent. It was observed that the addition of water caused some local coagulation of the dope which was left to stir till it became homogeneous again. This procedure was repeated till the dope became permanently turbid. 93 wt % of the amount of water required to cause phase separation was added to each dope (coagulation value).

Hollow Fiber Spinning of Hollow Fiber Membrane Substrates. The hollow fiber membrane substrates were prepared via a dry-jet wet spinning process employing an advanced coextrusion technology using a dual-layer spinneret. Polymer solutions were prepared according to the concentrations as described in Table S1 of Supporting Information (SI). The spinning parameters as well as the membrane post-treatment and module fabrication are described in the SI.

Interfacial Polymerization for Fabrication of TFC-FO Hollow Fiber Membranes. The M-phenylenediamine (MPD) solution in aqueous phase and trimesoyl chloride (TMC) solution in the organic phase were brought into contact leading to the formation of a polyamide layer through interfacial polymerization. Interfacial polymerization was performed on the lumen side of hollow fibers. The reactant solutions were pumped into the lumen side by a peristaltic pump with a flow rate of 3.5 mL/min from the bottom to top of the module held in a vertical hmmand 0.1 wt % sodium dodecyl sulfate (SDS) was fed to the lumen side of hollow fibers for 5 min.

After that, the excess MPD residual solutions/droplets were removed by purging a sweeping air for 5 min using a compressed air gun. Then a 0.15 wt % TMC-solution in hexane was brought into contact with the MPD saturated on the membrane's inner surface, leading to form a thin film of polyamide (PA) as a selective inner layer of hollow fibers. Subsequently, a purged sweeping air was applied for 1 min with an attempt to remove the residual solvents/droplets after the IP reaction. The resultant TFC membranes were heat-cured at 65 °C in an oven for 15 min and subsequently rinsed with DI water several times and stored in DI water before further characterizations.

Characterizations of Sulfonated PPSU Hollow Fiber Substrates and TFC-FO Membranes. The fabricated hollow fiber membrane substrate was first tested to measure its pure water permeability (PWP) (in L/m^2·bar.hr) by an ultrafiltration membrane permeation setup. Subsequently, the membrane was subjected to neutral solutes of progressively higher molecular weights (polyethylene glycol (PEG) or polyethylene oxide (PEO)) at 200 ppm to estimate its pore size, pore size distribution and molecular weight cutoff (MWCO) based on the solute transport method as elaborated more in the SI. The mass transport characteristics: water permeability, A, salt rejection R, and salt permeability of the TFC-FO hollow fiber membranes were also evaluated using the RO mode.

Pore Size and Pore Size Distribution. The fabricated hollow fiber membrane substrate was first tested to measure its pure water permeability (PWP) (in L/m^2·bar.hr) by an ultrafiltration membrane permeation setup. Subsequently, the membrane was subjected to neutral solutes of progressively higher molecular weights (polyethylene glycol (PEG) or polyethylene oxide (PEO)) separation tests by flowing them through the membrane's top surface under a pressure of 1 bar on the lumen side. Between runs of different solutes, the membrane was flushed thoroughly with DI water. The concentrations of the neutral solutes were measured by a total organic carbon analyzer (TOC ASI-5000A, Shimadzu, Japan). The measured feed (C_f) and permeate (C_p) concentrations were used for the calculation of the effective solute rejection coefficient R (%):

$$R = \left(1 - \frac{C_p}{C_f}\right) \times 100\% \quad (1)$$

In this work, solutions containing 200 ppm of different molecular weights of PEG or PEO were used as the neutral solutes for the characterizations of membrane pore size and

dx.doi.org/10.1021/es4013273 | Environ. Sci. Technol. 2013, 47, 7430−7436

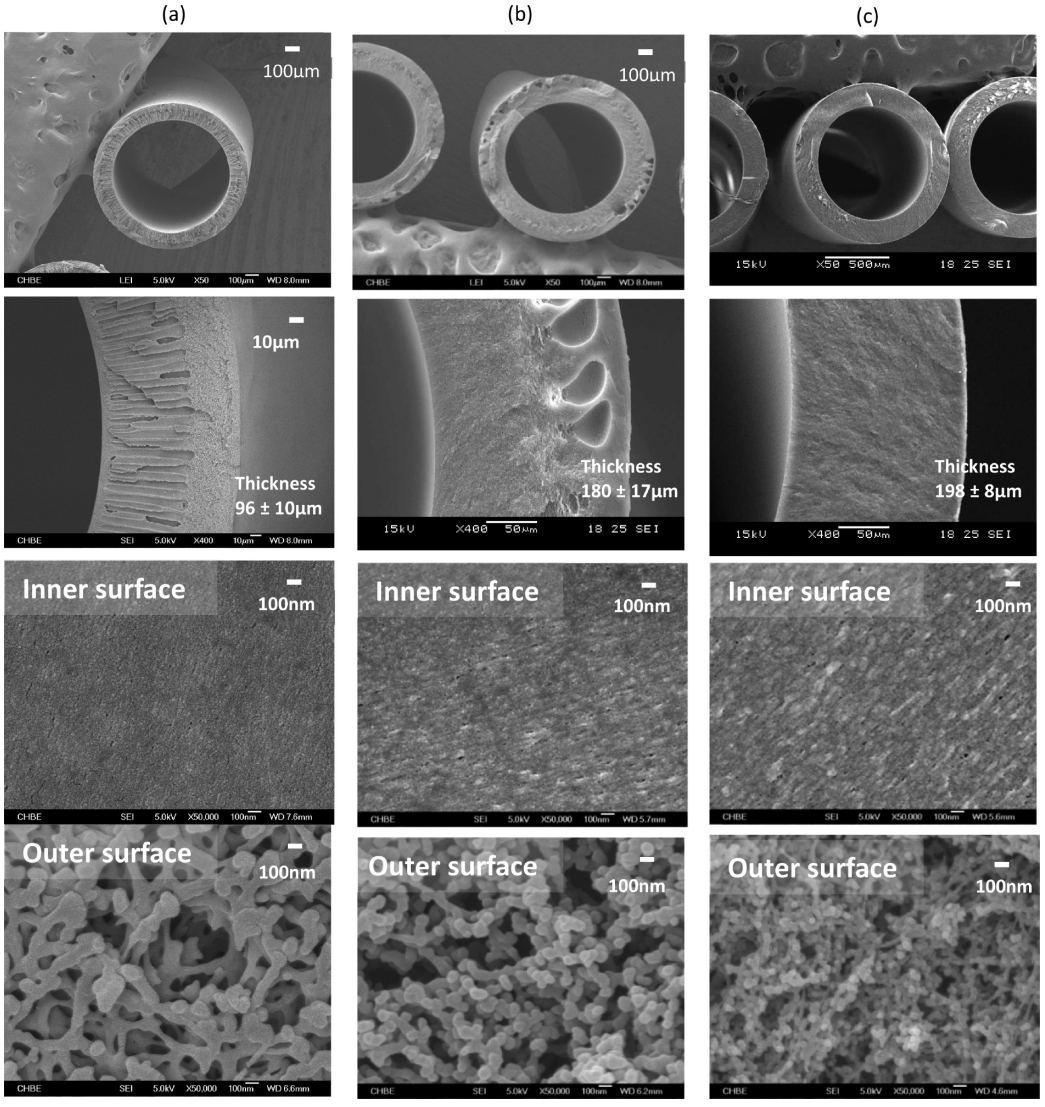

Figure 1. Morphology of membrane substrates fabricated from (a) PPSU; (b) 1.5 mol % sPPSU; and (c) 2.5 mol % sPPSU.

pore size distribution. The relationship between Stokes radius (r_s, nm) and molecular weight (Mw, gmol^{-1}) of these neutral solutes can be expressed as follows:

$$\text{for PEG: } r = 16.73 \times 10^{-12} \times M^{0.557} \quad (2)$$

$$\text{for PEO: } r = 10.44 \times 10^{-12} \times M^{0.587} \quad (3)$$

From eqs 2 and 3, the radius (r) of a hypothetical solute at a given Mw can be calculated. The mean effective pore size and the pore size distribution were then obtained according to the traditional solute transport approach by ignoring influences of the steric and hydrodynamic interaction between solute and membrane pores, the mean effective pore radius (μ_p) and the geometric standard deviation (σ_p) can be assumed to be the same as μ_s (the geometric mean radius of solute at R = 50%) and σ_g (the geometric standard deviation defined as the ratio of the r_s at R = 84.13% over that at R = 50%). Therefore, based on μ_p and σ_p, the pore size distribution of a membrane can be expressed as the following probability density function:

$$\frac{dR(d_p)}{dd_p} = \frac{1}{d_p \ln \sigma_p \sqrt{2\pi}} \exp\left[-\frac{(\ln d_p - \ln \mu_p)^2}{2(\ln \sigma_p)^2}\right] \quad (4)$$

Mass Transport Characteristics of TFC-FO Membranes. The water permeability and salt permeability of TFC-FO membranes were determined by testing the membranes under the RO mode. The water permeability coefficient (A) was obtained from the pure water permeation flux under the applied trans-membrane pressure of 1 bar. The salt rejection (R_s) was determined from the measured conductivities of permeate and feed by using feedwater containing 1000 ppm NaCl at 1 bar. The salt permeability coefficient (B), which is the intrinsic property of a membrane, was determined based on the solution-diffusion theory:[27]

$$\frac{1 - R_s}{R_s} = \frac{B}{A(\Delta P - \Delta \pi)} \quad (5)$$

Forward Osmosis Performance Tests. The forward osmosis experiments were carried out in a lab-scale cross-flow filtration unit. The feed and draw solutions were kept at room temperature of about 23 °C and fed cocurrently into the module. The flow rate at the lumen side was 0.1 L/min while that at the shell side was 0.2 L/min. Each membrane was tested under the PRO mode (active layer facing draw solution) and FO mode (active layer facing feed solution). The change in

dx.doi.org/10.1021/es4013273 | Environ. Sci. Technol. 2013, 47, 7430−7436

Table 1. Summary of Mean Effective Pore Size (μ_p), PWP, MWCO, and Contact Angles of TFC Membrane Substrates

membrane ID	μ_p (nm)	σ_p	MWCO (Da)	PWP (LMHbar^{-1})	contact angle (°)
PPSU	9.17 ± 0.52	1.52 ± 0.09	62319 ± 3205	150.1 ± 20.2	90.0 ± 4.7
1.5 mol % sPPSU	6.31 ± 0.35	1.67 ± 0.08	39731 ± 1753	213.4 ± 9.6	69.3 ± 1.8
2.5 mol % sPPSU	9.11 ± 0.41	1.65 ± 0.11	73877 ± 5139	238.7 ± 8.1	63.4 ± 4.2

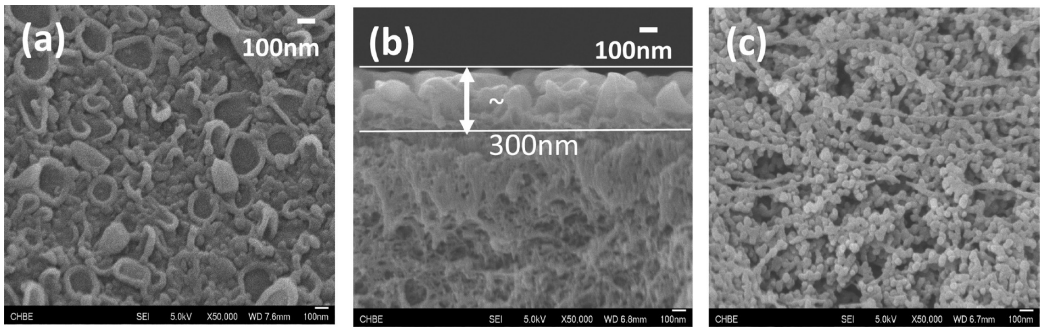

Figure 2. Morphology of 2.5% mol sPPSU TFC membranes after interfacial polymerization (a) inner surface; (b) edge of TFC layer; (c) outer surface.

feed solution weight was monitored by a computer connected to a balance (EK-4100i, A&D Company Ltd., Japan).

The water flux (Lm^{-2}h^{-1}, abbreviated as LMH) is calculated as follows:

$$J_v = \frac{\Delta V}{A.\ \Delta t} \tag{6}$$

Where ΔV (L) is the permeation water collected over a predetermined time Δt (h) in the FO process duration; A is the effective membrane surface area (m^2).

The salt concentration in the feedwater was determined from the conductivity measurement using a calibration curve for the single salt solution. The salt leakage or salt reverse-diffusion from the draw solution to the feed, J_s in g m^{-2} h^{-1} (abbreviated as gMH), is thereafter determined from the increase of the feed conductivity:

$$J_s = \frac{\Delta V(C_t V_t)}{A\cdot\Delta t} \tag{7}$$

where C_t and V_t are the salt concentration and the volume of the feed at the end of FO tests, respectively.

The water flux in FO processes can be modeled by the following equations[28]

For the PRO mode:

$$J_w = \frac{1}{K_m}\ln\frac{A\pi_{D,m} - J_w + B}{A\pi_{F,b} + B} \tag{8}$$

For the FO mode:

$$J_w = \frac{1}{K_m}\ln\frac{A\pi_{D,b} + B}{A\pi_{F,m} + J_w + B} \tag{9}$$

Where $\pi_{D,b}$ and $\pi_{F,b}$ refer to the osmotic pressures in the respective bulk draw and feed solutions, respectively, while $\pi_{D,m}$ and $\pi_{F,m}$ are the corresponding osmotic pressures on the membrane surfaces facing the draw and feed solutions, respectively. The relationship among solute diffusion resistivity K_m, within the porous layer, diffusivity D_s, membrane structural parameter S, membrane tortuosity τ, membrane thickness l, and membrane porosity ε can be represented as follows:

$$K_m = \frac{S}{D_s} = \frac{l\tau}{\varepsilon D_s} \tag{10}$$

The membrane structural parameter S is an intrinsic membrane property indicative of the degree of internal concentration polarization and a decrease in S positively influences the FO performance of membranes.

RESULTS AND DISCUSSION

Phase Separation Properties. It can be observed in Figure S1 of SI that as the degree of sulfonation of the PPSU polymer increases, a higher amount of water is needed to induce phase separation. In other words, it can be inferred that an increase in the degree of sulfonation in the dope system results in a slower phase inversion rate. Though the increase in sulfonation degree requires a larger amount of water to lead to phase separation, this increment in water addition is relatively small.

Characteristics and Performance of Membrane Substrates before Interfacial Polymerization. It is known that the degree of sulfonation of polymers used for membrane fabrication can influence the morphology, pore size, and pore size distribution as well as water permeability. This influence on morphology is well-exemplified as observed in Figure 1.

The hollow fibers fabricated from nonsulfonated polyphenylenesulfone display numerous finger-like macrovoids throughout the entire wall thickness due to instantaneous demixing. Strathmann[29] found a close correlation between membrane structure and precipitation rate. In general, systems with fast precipitation rates tend to form finger-like structure, whereas systems with slow precipitation rates result in sponge-like structure. On the other hand, the membrane substrate fabricated from 2.5 mol % sPPSU exhibits a fully sponge-like structure with no macrovoids and this can be attributed to the delayed demixing phenomenon induced by the sulfonated material. In summary, the degree of sulfonation has a direct impact on the amount of macrovoids formed, following the order of PPSU > 1.5 mol % sPPSU > 2.5 mol % sPPSU. The occurrence of macrovoids can also be linked to the viscosity of the dope solutions. The PPSU dope, with the lowest viscosity at 3−4 folds smaller than the sPPSU dopes as listed in Table S3

dx.doi.org/10.1021/es4013273 | Environ. Sci. Technol. 2013, 47, 7430−7436

Table 2. PRO and FO Performance of TFC-FO Hollow Fiber Membranes using a 0.5M NaCl Draw Solution

	PRO mode			FO mode		
membrane ID	water flux (LMH)	salt reverse flux (gMH)	J_s/J_w (g/L)	water flux (LMH)	salt reverse flux (gMH)	J_s/J_w (g/L)
TFC PPSU	22.64 ± 2.5	7.73 ± 0.51	0.34	12.37 ± 1.2	2.69 ± 0.21	0.22
TFC 1.5 mol % sPPSU	49.39 ± 6.2	11.00 ± 1.36	0.22	22.51 ± 2.3	5.49 ± 0.35	0.24
TFC 2.5 mol % sPPSU	37.71 ± 1.76	6.98 ± 0.71	0.19	17.98 ± 0.17	2.63 ± 0.32	0.15

Table 3. Transport Properties and Structural Parameters of TFC-FO Hollow Fiber Membranes

membrane ID	water permeability, A ($Lm^{-2}h^{-1}bar^{-1}$)	salt rejection[a] (%)	salt permeability, B ($Lm^{-2}h^{-1}$)	K_m (sm^{-1})	S^b (m)
TFC PPSU	3.15 ± 0.07	86.8 ± 0.7	0.0952 ± 0.003	5.07×10^5	7.46×10^{-4}
TFC 1.5 mol % sPPSU	1.99 ± 0.02	90.9 ± 0.3	0.0399 ± 0.002	1.11×10^5	1.63×10^{-4}
TFC 2.5 mol % sPPSU	1.80 ± 0.11	87.9 ± 0.9	0.0490 ± 0.011	1.63×10^5	2.40×10^{-4}

[a]Tested at 1 bar with 1000 ppm NaCl solution. [b]Structural parameters were calculated based on experiments under the FO mode using 0.5 M NaCl as draw solution and DI water as feed.

of SI, facilities a higher degree of nonsolvent intrusion during phase inversion and tends to form the most macrovoids. In addition, it can be observed that the reduction in phase inversion kinetics induced by the sulfonation leads to an increase hollow fiber wall thickness. Comparing PPSU and sPPSU hollow fibers, the sPPSU fibers have thicker walls as longer durations for phase inversion are allowed for the nascent membranes to adjust their thicknesses and more NMP solvent can flow out before the membrane contour is fixed.[30] The surface on the lumen side of hollow fibers exhibit relatively smaller pores as compared to the surface on the shell side which possesses a highly porous morphology with numerous large pores.

Table 1 and Figure S2 of SI show the PWP and pore size characteristics of the TFC membrane substrates fabricated from polymers of different degrees of sulfonation. As observed, increasing the degree of sulfonation of the membrane substrate increases the PWP. This is consistent with the values of contact angles which verify the increase in hydrophilicity along with sulfonation degree. It has been shown that better hydrophilicity facilities water transport.[31,32] Comparing 1.5 mol % and 2.5 mol % sPPSU membrane substrates, the latter has larger pores of 9.11 nm as compared to 6.31 nm of the former. At identical spinning conditions, the 2.5 mol % sPPSU polymer gives membrane substrates with a relatively larger pore size due to the delayed mixing phenomenon as discussed previously.

Characteristics and Performance of TFC-FO Hollow Fiber Membranes. Figure 2 depicts the typical polyamide layer of the TFC-FO hollow fiber membranes after interfacial polymerization was performed on the membrane substrates. A uniform layer of about 300 nm comprising ridges and valleys covers the inner selective side of the hollow fiber.

The fabricated TFC-FO membranes were evaluated for their performance under the PRO and FO mode using DI water as the feed and 0.5 M NaCl as the draw solution. The results are summarized in Table 2. The TFC-FO membranes fabricated from sPPSU substrates show relatively higher water fluxes than that fabricated from PPSU substrate, with a slight increase in salt reverse flux displayed by TFC 1.5 mol % sPPSU. This increase in water flux can be attributed to the increase in hydrophilicity of the substrate which aids in water transport through the substrate.

Among the results, according to the J_s/J_w values, the TFC 2.5 mol % sPPSU membrane exhibits the best performance with water fluxes of 37.7 and 18.0 LMH with relatively low reverse salt fluxes of 7.0 and 2.6 gMH for PRO and FO modes, respectively. Referring back to Table 1 as discussed previously, the PPSU substrate possesses almost similar pore size and MWCO as the 2.5 mol % sPPSU substrate. Therefore, while maintaining similar substrate characteristics, the effect of sulfonation can be more clearly demonstrated. Comparing TFC 2.5 mol % sPPSU with PPSU membranes, the water flux increases by more than 66%, whereas the reverse salt flux remains almost constant. It is evident that sulfonation plays an important role in enhancing water fluxes of TFC-FO membranes. The TFC membrane synthesized on the 1.5 mol % sPPSU substrate displays a higher water flux than that on 2.5 mol % sPPSU. This may be attributed to the higher degree of swelling of the 2.5 mol % sPPSU substrate, hence leading to a lower water flux. The degree of swelling for PPSU, 1.5 mol % sPPSU and 2.5 mol % sPPSU are 254.1 ± 8.3%, 269.5 ± 10.4%, and 298.5 ± 4.5%, respectively.

The water and salt permeabilites obtained from the pressurized tests in Table 3 are in good correlation with the FO data in Table 2. Table 3 summarizes the basic transport properties of the three various TFC-FO hollow fiber membranes. The water permeability of the TFC PPSU is comparatively higher that than of the TFC sPPSU hollow fiber membranes due to the presence of macrovoids and shows a relatively lower salt rejection rate. The values for both the sulfonated TFC membranes are relatively similar. The calculated structural parameter (S) significantly decreases when a sulfonated substrate replaces a nonsulfonated substrate. This implies that a lower internal concentration polarization effect can be achieved when sulfonated materials are used for the membrane substrates. This diminishing effect of internal concentration polarization is evident from the increase in water fluxes in both the PRO and FO modes. In short, a decrease in structural parameter (S) has been substantiated to contribute to a higher water flux from the comparison between the TFC PPSU and TFC 1.5 mol % and 2.5 mol % sPPSUs.

The TFC-FO membranes fabricated on the 1.5 mol % sPPSU substrate possesses the lowest structural parameter (S) and hence was chosen for further evaluation of the effect of increasing draw solution concentration on water flux. As seen in SI Figure S3, the increase in draw solution concentration from 0.5 to 2.0 M NaCl leads to an increase in water flux in both the PRO and FO modes. This is attributed to the increase in effective osmotic pressure difference. Another interesting observation is that the water flux in the PRO mode increases steadily with the increase in draw solution concentration while that of the FO mode increases at a much slower rate. This

phenomenon is indicative of the onset of ICP within the porous support layer which is more severe in the case of FO mode.

Osmotic Seawater Desalination. The newly developed TFC 1.5 mol % sPPSU FO hollow fiber membranes were chosen for characterization for its potential for seawater desalination. 3.5 wt % NaCl was used as a model for seawater solution to test the membrane performance, along with 2.0 M NaCl solution as the draw solution under the PRO mode.

Table 4 summarizes the water flux as a function of module length. Interestingly, the water flux increases with a decrease in module length. This is due to the effects of ICP and external concentration polarization (ECP) on the effective osmotic driving force across the membrane in the hollow fiber configuration. In other words, the 2.0 M NaCl draw solution is quickly diluted inside the membrane due to high water inflow, while the seawater concentration near the TFC layer is quickly built up. As a result, the osmotic driving force across the TFC layer is severely reduced. However, both ICP and ECP effects can be effectively mitigated by reducing the fiber length. The TFC 1.5 mol % sPPSU with a short fiber length exhibits water production of 22 LMH which is among the best in literature to date. In addition, a quick comparison to commercial HTI membranes[33] and other data found from literature as shown in Figure 3 shows that the TFC-FO hollow fiber membranes fabricated in this work surpasses that of HTI's and many others. Clearly, this work establishes the potential prospect of using sulfonated polyphenylenesulfone as a new material for substrates for TFC-FO hollow fibers fabricated from interfacial polymerization and provides useful insights in applying such membranes for real industrial applications.

Table 4. TFC Hollow Fiber Membranes Synthesized on 1.5 mol % sPPSU for Seawater Desalination[a]

membrane ID	fiber length (cm)	flux (LMH)
1	13.5	14.01 ± 0.05
2	10.3	16.23 ± 0.12
3	8.5	22.13 ± 1.21

[a]Under the PRO mode using a model seawater of 3.5 wt % NaCl and a 2.0 M NaCl solution as the draw solution.

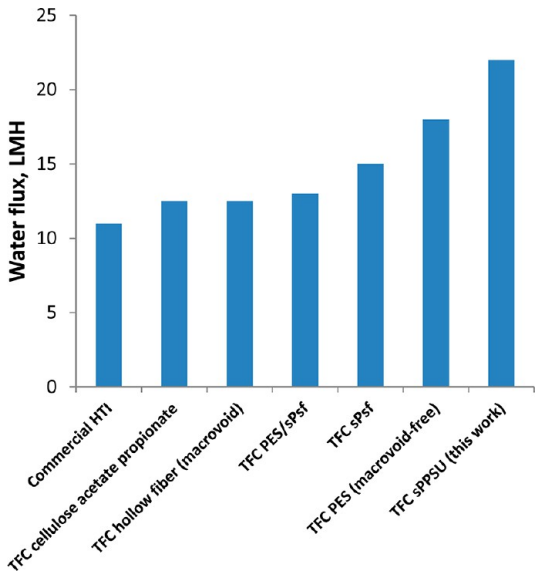

Figure 3. A comparison of water fluxes reported in literature for FO seawater desalination applications. Model seawater (3.5 wt % NaCl) solution was used as the feed solution, whereas 2.0 M NaCl as the draw solution. Commercial HTI,[33,34] cellulose acetate propionate,[16] TFC hollow fiber (macrovoids),[18] TFC PES/sPsf,[15] TFC sPsf,[21] TFC PES (macrovoid-free).[20].

■ ASSOCIATED CONTENT

Supporting Information

Materials; procedures for hollow fiber spinning, spinning parameters, membrane post-treatment and module fabrication; characterization techniques such as FESEM, viscosity. This material is available free of charge via the Internet at http://pubs.acs.org.

■ AUTHOR INFORMATION

Corresponding Author

*Phone: (65) 6516 6645; fax: (65) 6779 1936; e-mail: chencts@nus.edu.sg.

Notes

The authors declare no competing financial interest.

■ ACKNOWLEDGMENTS

We thank BASF SE, Germany for funding this work with a grant number of R-279-000-363-597. Thanks are due to Ms. Li Xue, Dr. Panu Sukitpaneenit and their help and suggestions to this work. This research was also partially funded by the Singapore National Research Foundation under its Competitive research Program for the project entitled, "Advanced FO Membranes and Membrane Systems for Wastewater Treatment, Water Reuse and Seawater Desalination" (grant number: R-279-000-336-281).

■ REFERENCES

(1) Shannon, M. A.; Bohn, P. W.; Elimelech, M.; Georgiadis, J. G.; Marinas, B. J.; Mayes, A. M. Science and technology for water purification in the coming decades. *Nature* **2008**, *452* (7185), 301−310.

(2) Semiat, R. Energy issues in desalination processes. *Environ. Sci. Technol.* **2008**, *42* (22), 8193−8201.

(3) Zhao, S.; Zou, L.; Tang, C. Y.; Mulcahy, D. Recent developments in forward osmosis: Opportunities and challenges. *J. Membr. Sci.* **2012**, *396* (0), 1−21.

(4) Zhao, S.; Zou, L.; Mulcahy, D. Effects of membrane orientation on process performance in forward osmosis applications. *J. Membr. Sci.* **2011**, *382* (1−2), 308−315.

(5) Lee, K. L.; Baker, R. W.; Lonsdale, H. K. Membranes for power generation by pressure-retarded osmosis. *J. Membr. Sci.* **1981**, *8* (2), 141−171.

(6) Achilli, A.; Cath, T. Y.; Childress, A. E. Power generation with pressure retarded osmosis: An experimental and theoretical investigation. *J. Membr. Sci.* **2009**, *343* (1−2), 42−52.

(7) Garcia-Castello, E. M.; McCutcheon, J. R.; Elimelech, M. Performance evaluation of sucrose concentration using forward osmosis. *J. Membr. Sci.* **2009**, *338* (1−2), 61−66.

(8) Jiao, B.; Cassano, A.; Drioli, E. Recent advances on membrane processes for the concentration of fruit juices: A review. *J. Food Eng.* **2004**, *63* (3), 303−324.

(9) Yang, Q.; Wang, K. Y.; Chung, T. S. A novel dual-layer forward osmosis membrane for protein enrichment and concentration. *Sep. Purif. Technol.* **2009**, *69* (3), 269−274.

(10) Chung, T. S.; Li, X.; Ong, R. C.; Ge, Q.; Wang, H.; Han, G. Emerging forward osmosis (FO) technologies and challenges ahead for clean water and clean energy applications. *Curr. Opin. Chem. Eng.* **2012**, *1* (3), 246−257.

(11) Li, Z. Y.; Yangali-Quintanilla, V.; Valladares-Linares, R.; Li, Q.; Zhan, T.; Amy, G. Flux patterns and membrane fouling propensity during desalination of seawater by forward osmosis. *Water Res.* **2012**, *46* (1), 195−204.
(12) Mi, B.; Elimelech, M. Organic fouling of forward osmosis membranes: Fouling reversibility and cleaning without chemical reagents. *J. Membr. Sci.* **2010**, *348* (1−2), 337−345.
(13) Veríssimo, S.; Peinemann, K. V.; Bordado, J. Thin-film composite hollow fiber membranes: An optimized manufacturing method. *J. Membr. Sci.* **2005**, *264* (1−2), 48−55.
(14) Shintani, T.; Matsuyama, H.; Kurata, N. Development of a chlorine-resistant polyamide reverse osmosis membrane. *Desalination* **2007**, *207* (1−3), 340−348.
(15) Wang, K. Y.; Chung, T. S.; Amy, G. Developing thin-film-composite forward osmosis membranes on the PES/SPSf substrate through interfacial polymerization. *AIChE J.* **2012**, *58* (3), 770−781.
(16) Li, X.; Wang, K. Y.; Helmer, B.; Chung, T. S. Thin-film composite membranes and formation mechanism of thin-film layers on hydrophilic cellulose acetate propionate substrates for forward osmosis processes. *Ind. Eng. Chem. Res.* **2012**, *51* (30), 10039−10050.
(17) Yip, N. Y.; Tiraferri, A.; Phillip, W. A.; Schiffman, J. D.; Elimelech, M. High performance thin-film composite forward osmosis membrane. *Environ. Sci. Technol.* **2010**, *44* (10), 3812−3818.
(18) Chou, S.; Shi, L.; Wang, R.; Tang, C. Y.; Qiu, C.; Fane, A. G. Characteristics and potential applications of a novel forward osmosis hollow fiber membrane. *Desalination* **2010**, *261* (3), 365−372.
(19) Wang, R.; Shi, L.; Tang, C. Y.; Chou, S.; Qiu, C.; Fane, A. G. Characterization of novel forward osmosis hollow fiber membranes. *J. Membr. Sci.* **2010**, *355* (1−2), 158−167.
(20) Sukitpaneenit, P.; Chung, T. S. High Performance thin-film composite forward osmosis hollow fiber membranes with macrovoid-free and highly porous structure for sustainable water production. *Environ. Sci. Technol.* **2012**, *46* (13), 7358−7365.
(21) Widjojo, N.; Chung, T. S.; Weber, M.; Maletzko, C.; Warzelhan, V. The role of sulphonated polymer and macrovoid-free structure in the support layer for thin-film composite (TFC) forward osmosis (FO) membranes. *J. Membr. Sci.* **2011**, *383* (1−2), 214−223.
(22) Shi, L.; Chou, S. R.; Wang, R.; Fang, W. X.; Tang, C. Y.; Fane, A. G. Effect of substrate structure on the performance of thin-film composite forward osmosis hollow fiber membranes. *J. Membr. Sci.* **2011**, *382* (1−2), 116−123.
(23) Zhang, G.; Song, X.; Ji, S.; Wang, N.; Liu, Z. Self-assembly of inner skin hollow fiber polyelectrolyte multilayer membranes by a dynamic negative pressure layer-by-layer technique. *J. Membr. Sci.* **2008**, *325* (1), 109−116.
(24) Geise, G. M.; Lee, H. S.; Miller, D. J.; Freeman, B. D.; McGrath, J. E.; Paul, D. R. Water purification by membrane: The role of polymer science. *J. Polym. Sci., Part B: Polym. Phys.* **2010**, *48* (15), 1685.
(25) Doi, S.; Hamanaka, K. Pore size control technique in the spinning of polysulfone hollow fiber ultrafiltration membranes. *Desalination* **1991**, *80* (2−3), 167−180.
(26) Liu, Y.; Koops, G. H.; Strathmann, H. Characterization of morphology controlled polyethersulfone hollow fiber membranes by the addition of polyethylene glycol to the dope and bore liquid solution. *J. Membr. Sci.* **2003**, *223* (1−2), 187−199.
(27) Loeb, S.; Mehta, G. D. A two-coefficient water transport equation for pressure-retarded osmosis. *J. Membr. Sci.* **1978**, *4* (0), 351−362.
(28) Mehta, G. D.; Loeb, S. Internal polarization in the porous substructure of a semipermeable membrane under pressure-retarded osmosis. *J. Membr. Sci.* **1978**, *4* (0), 261−265.
(29) Strathmann, H., Production of microporous media by phase inversion processes. In *Materials Science of Synthetic Membranes*; American Chemical Society: Washington, DC, 1985; Vol. *269*, pp 165−195.
(30) Xing, D. Y.; Peng, N.; Chung, T. S. Formation of cellulose acetate membranes via phase inversion using ionic liquid, [BMIM]-SCN, as the solvent. *Ind. Eng. Chem. Res.* **2010**, *49* (18), 8761−8769.
(31) Li, Y.; Chung, T. S.; Chan, S. Y. High-affinity sulfonated materials with transition metal counterions for enhanced protein separation in dual-layer hollow fiber membrane chromatography. *J. Chromatogr., A* **2008**, *1187* (1−2), 285−288.
(32) Rahimpour, A.; Madaeni, S. S.; Ghorbani, S.; Shockravi, A.; Mansourpanah, Y. The influence of sulfonated polyethersulfone (SPES) on surface nano-morphology and performance of polyethersulfone (PES) membrane. *Appl. Surf. Sci.* **2010**, *256* (6), 1825−1831.
(33) McCutcheon, J. R.; McGinnis, R. L.; Elimelech, M. Desalination by ammonia−carbon dioxide forward osmosis: Influence of draw and feed solution concentrations on process performance. *J. Membr. Sci.* **2006**, *278* (1−2), 114−123.
(34) Phillip, W. A.; Yong, J. S.; Elimelech, M. Reverse draw solute permeation in forward osmosis: Modeling and experiments. *Environ. Sci. Technol.* **2010**, *44* (13), 5170−5176.